DOI: 10.1002/adma.200502686

# Fast and Spatially Resolved Environmental Probing Using Stimuli-Responsive Polymer Layers and Fluorescent Nanocrystals**

By *Leonid Ionov*,* *Sameer Sapra*, *Alla Synytska*, *Andrey L. Rogach*, *Manfred Stamm*, and *Stefan Diez**

The development of chemical and biological sensors is of growing interest for many analytical applications, including the monitoring of environmental and industrial processes and the quality control of nutrition and water, as well as for medical and security purposes. In recent sensor approaches, the change in fluorescence of organic dyes or inorganic nanoparticles in different environments has been widely used to detect various ions and chemical substances.[1–12] In most of the cases, the environmental changes lead to quenching of the fluorescence[8–10] or to a shift of the emission spectrum due to energy transfer.[5,11,12] In such applications, semiconductor nanocrystals have several advantages over organic fluorescent dyes. In particular, nanocrystals have a high photostability, broad absorption spectra in combination with a narrow and symmetric emission band, and high molar absorbance.[5]

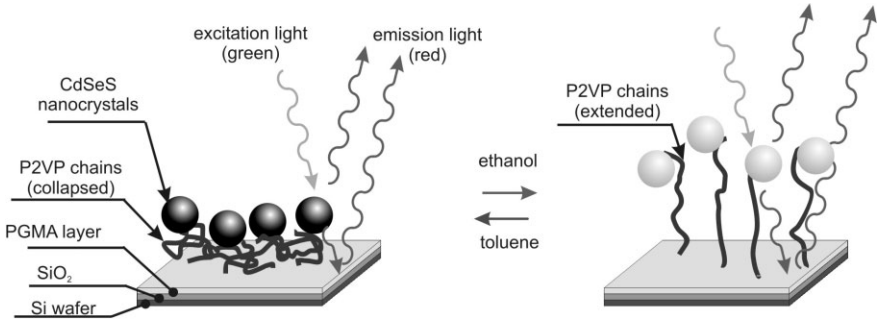


**Figure 1.** Schematic of the polymeric sensor. Hydrophobic nanocrystals are adsorbed on a stimuli-responsive polymer layer that was previously grafted onto a reflecting substrate. The nanocrystal–surface distance depends on the conformation of the polymer chains and changes in different solvents. The change in height is then reported by a variation in the detected fluorescence intensity.

Here, we report a novel approach for the design of environmental sensors based on fluorescence interference contrast (FLIC)[13] of semiconductor nanocrystals near a reflecting silicon surface (Fig. 1). FLIC arises from the interference between light that is directly emitted (or absorbed) by a nanoparticle and the light that is reflected by the mirror surface. Consequently, the intensity of the detected fluorescence light becomes a periodic function of the nanoparticle distance from the surface. The period of this function is determined by the wavelength of the light and the refractive index of the surrounding medium. Fluorescent nanoparticles located in close proximity to the mirror surface will appear dark, while particles about a quarter-wavelength away will appear with maximum brightness. Inserting a polymer layer, whose thickness depends on the environmental conditions, provides a simple and cheap strategy for the design of a sensor. Using the swelling behavior of a poly(2-vinyl pyridine) (P2VP) polymer layer anchored to a silica wafer, we use the sensor for precise measurements of solvent composition with unprecedented spatial and temporal resolution.

The P2VP polymer layer was grafted onto chips from a Si wafer with a native $SiO_2$ layer of thickness $H_{SiO_2} = 1.6$ nm (precoated with PGMA, $H_{PGMA} = 1.5$ nm, see Experimental). The thickness of the dry P2VP layer was measured by ellipsometry to be $H^{DRY} = 7.6\ \text{nm} \pm 0.5\ \text{nm}$, corresponding to a grafting density of about 0.1 chains $\text{nm}^{-2}$. Because the distance between the grafting points ($d = 3.5$ nm) was smaller than the gyration radius of the P2VP polymer coils ($R_g \approx 5$ nm), the polymer layer was considered brushlike. The surface of the P2VP layer was smooth with a root mean square roughness less than 0.3 nm, as measured by atomic force microscopy (AFM). We found that the P2VP brush undergoes a completely reversible change in thickness in different solvents. In toluene (a "poor" solvent), the polymer layer had a thickness of $H^{TOLUENE} = 9\ \text{nm} \pm 1\ \text{nm}$ while in ethanol (a "good" solvent) the P2VP brush swelled by a factor of about 2.5 to a thickness of $H^{ETHANOL} = 19.6\ \text{nm} \pm 1\ \text{nm}$ (values measured by ellipsometry without attached nanocrystals).

[*] Dr. L. Ionov, Dr. S. Diez
Max-Planck-Institute of Molecular Cell Biology and Genetics
01307 Dresden (Germany)
E-mail: ionov@mpi-cbg.de; diez@mpi-cbg.de
Dr. L. Ionov, Dr. A. Synytska, Prof. M. Stamm
Leibniz-Institute of Polymer Research
01069 Dresden (Germany)
Dr. S. Sapra, Dr. A. L. Rogach
Photonics and Optoelectronics Group
Physics Department and CeNS
Ludwig-Maximilians-Universität München
80799 München (Germany)

[**] We thank J. Kerssemakers and J. Helenius for help with the experimental work and J. Feldmann for helpful discussions, as well as K.-J. Eichhorn and R. Schulze for support with the ellipsometry. Andor Technology (Belfast, Northern Ireland) is greatly acknowledged for the generous loan of the high-speed EMCCD camera. The authors are grateful to the DFG (grant SPP 1164) and the BMBF (grant 03N8712) for financial support. S. Sapra is thankful to the Humboldt-Foundation for funding his research stay in Germany.

ADVANCED MATERIALS

Hydrophobic CdSeS nanocrystals (emitting at 570 nm, see Figs. 2a and b) were adsorbed from a 1 mM toluene solution onto the P2VP brush during 30 s. Non- or weakly adsorbed particles were removed by rinsing with toluene. Changes in the surface morphology (Fig. 2c) and the appearance of a fluorescence signal indicated the incorporation of nanocrystals into the polymer layer. While there was no chemical bonding between the nanocrystals and the polymer chains, the nanocrystals were held in the polymer matrix, most likely due to hydrophobic–hydrophobic interaction. Stability of this interaction was verified by an unchanged fluorescence intensity after rinsing the surface in various solvents and subsequent drying. Atomic force microscopy (AFM) images (Fig. 2c) showed that the nanocrystals covered approximately 5 % of the brush surface.

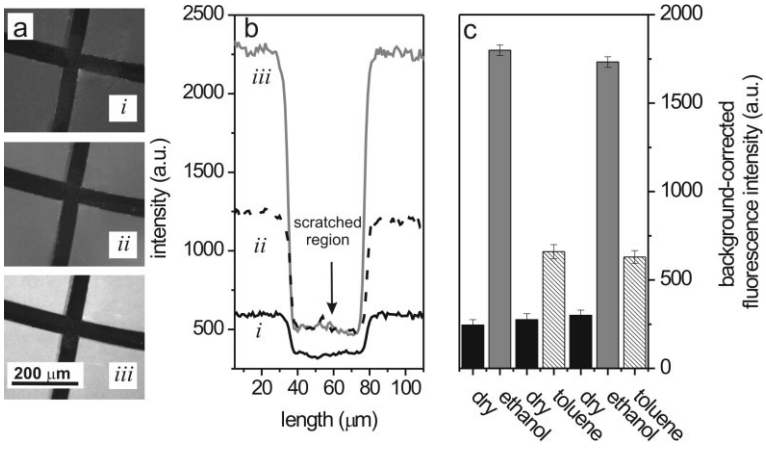


**Figure 3.** Fluorescence of the CdSeS–P2VP brush layer. a) Fluorescence microscopy images of the CdSeS–P2VP brush layer in the dry state (i), wetted with a droplet of toluene (ii), and wetted with a droplet of ethanol (iii). For contrast, thin stripes of the polymer–nanocrystal layer were removed using a diamond knife. b) Intensity profiles across one of the scratches in (a). c) Multiple cycles of solvent application and drying. Average intensity values are corrected for the background fluorescence measured in the scratched areas. Plotted are the average intensity values ± the standard deviation for areas of 200 μm × 200 μm.

We found that the fluorescence intensity of the CdSeS nanocrystals adsorbed onto the P2VP brush strongly depended on the surrounding solvent (Fig. 3). To show that the observed fluorescence changes are a measure of the changes in the P2VP layer thickness, the polymer–nanocrystal layer was partly removed by scratches with a diamond knife in a cross-like pattern. While the fluorescence intensity was low in a dry environment (Fig. 3a, i), the intensity increased significantly when a toluene droplet was deposited on the brush surface (Fig. 3a, ii). The increase in fluorescence intensity became even more pronounced when toluene was replaced by ethanol (Fig. 3a, iii). Intensity profiles across one of the scratches are given in Figure 3b. The slight increase in the fluorescence intensity in the scratched areas after depositing of toluene and ethanol was attributed to reflections of the fluorescent light within the liquid droplets. Notably, the solvent-induced switching of the fluorescence intensity was found to be completely reversible and reproducible. Figure 3c shows averaged values of the background-corrected fluorescence intensities for multiple cycles of solvent application and drying on the same chip. To rule out that the observed changes in fluorescence were the result of a chemical interaction of the solvent with the nanocrystals themselves we performed control experiments using the same layer system on glass. No dependence of the fluorescence intensity on the surrounding environment was found.

We investigated how well the intensity variations could be used to measure the thickness of polymer layers. For that, we performed measurements on a Si chip with four different thicknesses of $SiO_2$ (Fig. 4, method similar to one reported by Braun et al.).[14] The simultaneous recording of all four intensity signals allowed each individual environmental condition to be fit by the following equation:[15]

$$I(h) = I_0\left(2\cdot(1-r_f)^2+8r_f\sin^2\left(\frac{2\pi}{\lambda_{EX}}(n_{SiO_2}\cdot h_{SiO_2}+n\cdot h)\right)\right)\times\left(2\cdot(1-r_f)^2+8r_f\sin^2\left(\frac{2\pi}{\lambda_{EM}}(n_{SiO_2}\cdot h_{SiO_2}+n\cdot h)\right)\right) \quad (1)$$

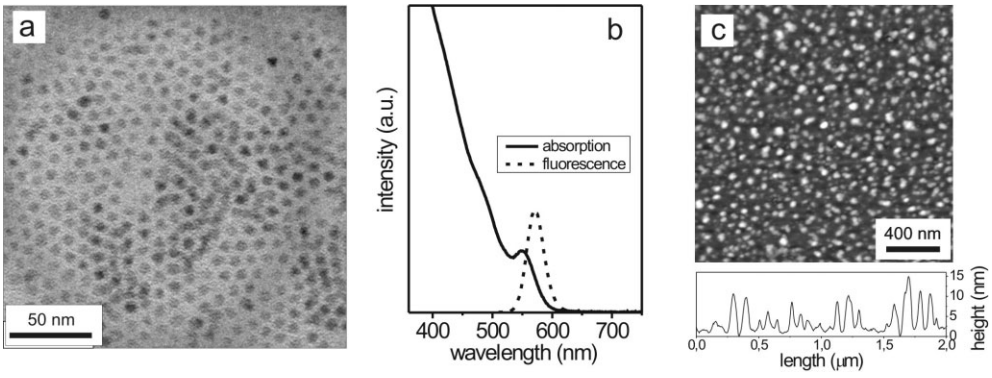


**Figure 2.** Characterization of the semiconductor nanocrystals. a) Transmission electron microscopy (TEM) image of the nanocrystals. b) Absorption and emission spectra of the nanocrystals. c) AFM image of the P2VP brush after adsorption of the nanocrystals.

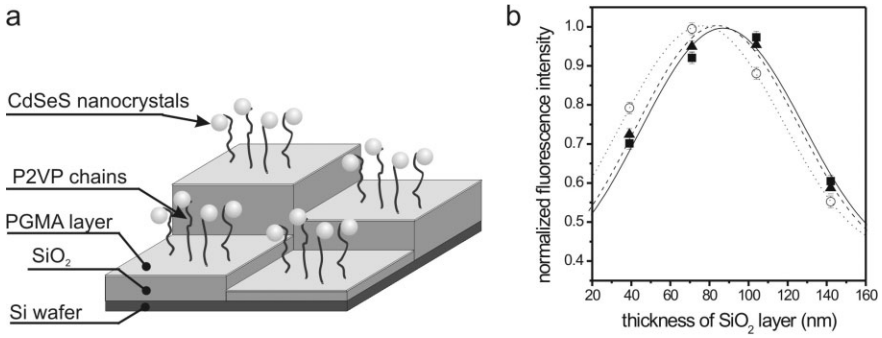


**Figure 4.** Quantification of the thickness of the polymer layer by FLIC. a) Schematic of the simultaneous intensity measurements at four different thicknesses of $SiO_2$. b) Normalized fluorescence intensity values of the CdSeS–P2VP brush layer on the $SiO_2$ steps: ■: dry sample, ▲: after deposition of the toluene droplet, ○: after deposition of the ethanol droplet. FLIC curves are fitted using Equation 1 for the dry sample (solid line), the sample in toluene (dashed line), and in ethanol (dotted line).

where $I_0$ serves as a proportionality factor. Refractive indices for the polymer layer and the $SiO_2$ layer are represented by $n$ and $n_{SiO_2} = 1.46$, respectively. $h_{SiO_2}$ is the oxide thickness and $h$ is the height above the oxide surface. The excitation and emission wavelengths, $\lambda_{EX}$ and $\lambda_{EM}$, are 565 nm and 610 nm, respectively. The reflection coefficient is represented by $r_f$.

In our fitting procedure using Equation 1 (Fig. 4b), we kept the refractive index of the polymer layer constant and equal to that obtained from the ellipsometric measurement (Table 1) while the other parameters ($r_f$, $I_0$, and $h$) were varied. For each environmental condition, we thus obtained a height value, $h$, which represents the distance between the nanocrystals and the $SiO_2$ surface. Note that the height values derived from our FLIC approach are nearly identical to the ellipsometric data (Table 1). The shift in the curves in Figure 4b represents the different contributions of the polymer layers to the absolute height of the nanocrystals above the reflecting $Si/SiO_2$ interface.

**Table 1.** Values of the parameters as obtained by fitting the experimental data of Figure 4 using Equation 1. Also included is the ellipsometry data as obtained for the polymer layers without nanocrystals. The thickness of the polymer layer represents the sum of the thickness of the anchoring PGMA layer and the thickness of the P2VP grafted layer. The typical error in the determination of the polymer layer using ellipsometry is ±1 nm.

| Conditions | FLIC | | | | Ellipsometry |
|---|---|---|---|---|---|
| | $I_0$ | $r_f$ | $h$ [nm] | $n$ | $H_{PGMA}+H_{P2VP}$ [nm] |
| Ethanol | 39.8 | 0.11 | 20.9 | 1.46 | 21.1 |
| Toluene | 37.0 | 0.11 | 12.1 | 1.58 | 10.5 |
| Dry | 37.0 | 0.11 | 9.1 | 1.59 | 9.1 |

We performed two specific experiments in order to demonstrate the applicability of the presented polymer–nanocrystal system for environmental sensing. In the first experiment we utilized the CdSeS–P2VP brush layer for sensing the composition of liquid mixtures. As the conformation of the individual polymer chains will gradually depend on the mixing ratio between a "good" and a "poor" solvent, the thickness of the polymer layer should also vary between the extremes, as determined above for ethanol and toluene. In fact, we did find a strongly linear relationship between the observed fluorescence intensity of our sensor system and the ethanol–toluene mixing ratio (Fig. 5a). Using this plot as calibration, the composition of an unknown ethanol–toluene mixture can be determined easily. In the second experiment, we demonstrated the applicability of the polymer–nanocrystal system for the real-time monitoring of liquid flow. For that purpose we constructed a flow chamber (width 2 mm, height 50 μm) consisting of a glass cover slip on one side and a Si chip with the polymer–nanocrystal system on the other. We then recorded on a charge-coupled device (CCD) camera (image acquisition with 100 frames per second) how the front of an ethanol droplet fills such a closed channel (Fig. 5b). While the dry area on the surface appears

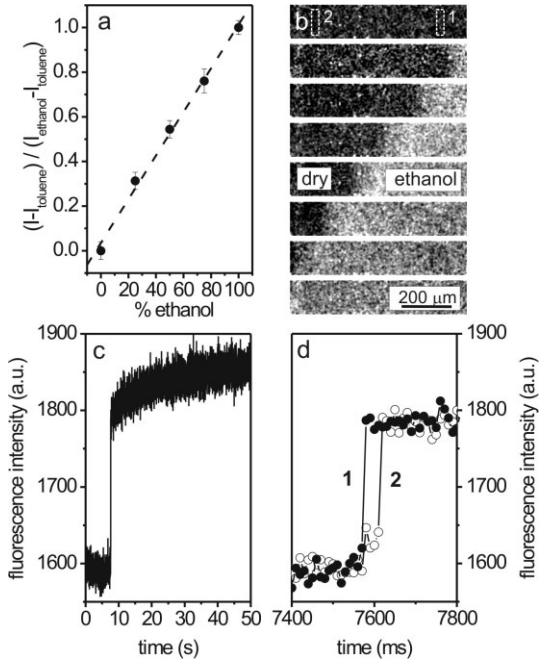


**Figure 5.** Sensory applications of P2VP–CdSeS layers. a) Dependence of the normalized fluorescence intensity $(I - I_{toluene})/(I_{ethanol} - I_{toluene})$ as a function of the ethanol content in the toluene–ethanol mixture. $I_{toluene}$ and $I_{ethanol}$ denote the measured intensities for 100% toluene or ethanol, respectively. b) Sequence of fluorescence microscopy images during ethanol perfusion (from the right) into a flow cell with a P2VP–CdSeS layer. The time interval between consecutive images is 10 ms. c,d) Time-dependence of the detected fluorescence intensity from (b) over 50 s at location 1 and over 400 ms at locations 1 and 2. It can be observed that the P2VP–CdSeS layer responds within less than 10 ms. The flow rate of the solvent inside the channel was 0.015 m $s^{-1}$.

  

ADVANCED MATERIALS

dark, the part of the surface that is wetted by ethanol shows an increased intensity due to the increased distance of the nanocrystals from the surface.

Although complete switching of the P2VP–CdSeS layer finishes after about 1–3 min of swelling, the first sharp response of the signal occurs in less than 10 ms (Figs. 5c and d). Thus, this very fast response of the polymer layers will allow the use of the polymer–nanocrystal layers for ultrafast sensing and for the dynamic investigation of the properties of polymer grafted layers in contact with liquids or other surfaces.

Although other methods, such as imaging ellipsometry, allow the precise mapping of the properties of thin films, the present method has distinct advantages. Using a high-speed camera, we demonstrated the possibility to acquire 100 spatially resolved images per second and even faster data acquisition is possible. On the contrary, the typical acquisition time associated with imaging ellipsometry is about 1 min. Moreover, if spatial information is not required, the detection system can be reduced to a light-emitting diode for fluorescence excitation and a photodiode for emission measurements. A simple and compact sensor should be realizable. The main factors that limit the applicability of our sensor are related to the chemical stability of the polymer layer and the nanocrystals. For example, we found that the CdSeS nanocrystals used in our experiments decomposed at < pH 3. Concerning the thickness of the used polymer layers we note that the difference between the compacted and swollen state is required to be less than 120 nm (half the period of the FLIC curve). However, the actual position on the periodic FLIC curve can be tuned by the thickness of the underlying $SiO_2$ layer.

To conclude, we have developed a novel strategy for the design of fluorescent environmental sensors. Our method is based on nanocrystals incorporated into polymer layers grafted onto reflecting surfaces. The main advantages of our approach are extreme instrumental simplicity, high spatial precision of the measurements and a fast signal response. We foresee a large potential of such sensors for the in situ monitoring of mixing and separation processes, as well as for the control of the composition of liquid mixtures in microfluidic devices. Our sensing strategy can be extended to aqueous environments when appropriate polymers are used. For example, polyelectrolyte layers are responsive to pH and ionic strength, while poly(*N*-isopropyl acrylamide) is sensitive to temperature. In addition, we believe that our method can contribute to a further understanding of the dynamic properties of ultrathin polymer films and their interaction with environmental components ranging from ions and inorganic nanoparticles to proteins and cells.

## *Experimental*

Highly polished single-crystal silicon wafers of {100} orientation with either 1.8 nm or 148 nm thick silicon oxide layers (Semiconductor Processing Co) were used as substrates. The wafers were cleaned with chloroform in an ultrasonic bath for 30 min, placed in piranha solution (3:1 concentrated sulfuric acid and 30 % hydrogen peroxide) for 1 h, and rinsed several times with water. Polyglycidylmethacrylate (PGMA) (number-average molecular weight, $M_n = 84\,000$ g mol$^{-1}$) was synthesized by free radical polymerization of glycidyl methacrylate (Aldrich). Carboxyl-terminated poly(2-vinyl pyridine) (P2VP-COOH, $M_n = 39\,200$ g mol$^{-1}$, weight-average molecular weight, $M_w = 41\,500$ g mol$^{-1}$) was purchased from Polymer Source, Inc. The silicon wafers with patches of silicon oxide of different thicknesses were prepared using step-by-step etching in 10 % HF [14].

P2VP brush layers were prepared via a two-step procedure [16]. In brief, a thin layer of PGMA (ca. 1.5 nm) was deposited by spin-coating from a 0.01 % solution in chloroform and annealed at 110 °C for 5 min. On top, a thin film of P2VP-COOH (2 % solution in chloroform) was spin-coated and annealed for 5 h at 150 °C. Ungrafted polymer was removed using Soxhlet extraction in chloroform for 3 h.

Hydrophobic CdSeS nanocrystals were prepared by the method described in the literature [17]. Typically, CdO (0.05 g), oleic acid (0.46 g), and 15 mL tri-*n*-octylamine were mixed in a three-necked flask and heated to 300 °C under inert atmosphere. A solution of Se (0.0021 g) and S (0.0124 g) in 1 mL tri-*n*-octylphosphine was swiftly injected into the hot solution and the reaction was allowed to proceed for 5 min. This leads to bright-orange emitting nanocrystals (quantum yield ca. 50 %) with a narrow size distribution as is seen in the TEM images in Figure 2a. The average particle size is 4.8 nm. By varying the Se/S ratio nanocrystals with emissions ranging between violet and red can be prepared.

The thickness of polymer layers in the dry state was measured at $\lambda = 632.8$ nm and an angle of incidence of 70° with a null-ellipsometer in a polarizer compensator–sample analyzer (Multiscope, Optrel Berlin) as described elsewhere [18,19]. From the obtained values, we calculated the distance between grafting points by the following equation:

$$d = (H\,\rho\,N_A/M_w)^{-1/2} \quad (2)$$

where $H$ is the ellipsometric thickness, $\rho$ is the mass density (for simplicity we used $\rho = 1$ g cm$^{-3}$), $N_A$ is Avogadro's number, and $M_w$ is the molecular weight. "In situ" ellipsometric measurements were performed to examine the swelling behavior of the polymer brush in different media. An ellipsometric cell with thin glass walls fixed at a known angle (68°) from the sample plane was used [20].

AFM studies were performed with a Dimension 3100 (Digital Instruments, Inc., Santa Barbara, CA) microscope. Tapping mode was used to map the film morphology at ambient conditions. We estimated the surface coverage of adsorbed nanocrystals by the following equation:

$$\varphi = 100\,\%\;N\,\pi\,d^2/4A \quad (3)$$

where $d$ is the diameter of the nanocrystals and $N$ is the number of nanocrystals detected per area $A$.

Fluorescence images were obtained using an Axiovert 200M inverted microscope with a 10× objective (Zeiss, Oberkochen, Germany). For data acquisition (Figs. 3 and 4) a CoolSnap HQ Camera (Photometrics, Tucson, AZ) was used in conjunction with a MetaMorph imaging system (Universal Imaging, Downingtown, PA). The data in Figure 5 were obtained using an iXon DV 887-BI electron-multiplied CCD camera (Andor Technology, Belfast, Northern Ireland). The following filter set was used for imaging: Excitation: HQ 535/50, Dichroic: Q 565 LP, Emission: HQ 610/75 (Chroma Technology, Rockingham, VT).

Received: December 15, 2005
Final version: February 21, 2006
Published online: April 26, 2006

[1] H. A. Ho, M. Bera-Aberem, M. Leclerc, *Chem. Eur. J.* **2005**, *11*, 1718.
[2] R. Nutiu, Y. Li, *Chem. Eur. J.* **2004**, *10*, 1868.

  

[3] N. L. Rosi, C. A. Mirkin, *Chem. Rev.* **2005**, *105*, 1547.
[4] A. P. de Silva, H. Q. Gunaratne, T. Gunnlaugsson, A. J. M. Huxley, C. P. McCoy, J. T. Rademacher, T. E. Rice, *Chem. Rev.* **1997**, *97*, 1515.
[5] I. L. Medintz, H. T. Uyeda, E. R. Goldman, H. Mattoussi, *Nat. Mater.* **2005**, *4*, 435.
[6] E. Pringsheim, D. Zimin, O. S. Wolfbeis, *Adv. Mater.* **2001**, *13*, 819.
[7] A. Ueno, *Adv. Mater.* **1993**, *5*, 132.
[8] C. Bo, Y. Ying, Z. Zhentao, Z. Ping, *Chem. Lett.* **2004**, *33*, 1608.
[9] Y. F. Chen, Z. Rosenzweig, *Anal. Chem.* **2002**, *74*, 5132.
[10] S. Westenhoff, N. A. Kotov, *J. Am. Chem. Soc.* **2002**, *124*, 2448.
[11] E. R. Goldman, I. L. Medintz, J. L. Whitley, A. Hayhurst, A. R. Clapp, H. T. Uyeda, J. R. Deschamps, M. E. Lassman, H. Mattoussi, *J. Am. Chem. Soc.* **2005**, *127*, 6744.
[12] I. L. Medintz, E. R. Goldman, M. E. Lassman, J. M. Mauro, *Bioconjugate Chem.* **2003**, *14*, 909.
[13] A. Lambacher, P. Fromherz, *Appl. Phys. A* **1996**, *63*, 207.
[14] D. Braun, P. Fromherz, *Appl. Phys. A* **1997**, *65*, 341.
[15] Y. Kaizuka, J. T. Groves, *Biophys. J.* **2004**, *86*, 905.
[16] I. Tokareva, S. Minko, J. H. Fendler, E. Hutter, *J. Am. Chem. Soc.* **2004**, *126*, 15 950.
[17] E. Jang, S. Jun, L. Pu, *Chem. Commun.* **2003**, 2964.
[18] S. Minko, S. Patil, V. Datsyuk, F. Simon, K. J. Eichhorn, M. Motornov, D. Usov, I. Tokarev, M. Stamm, *Langmuir* **2002**, *18*, 289.
[19] L. Ionov, B. Zdyrko, A. Sidorenko, S. Minko, V. Klep, I. Luzinov, M. Stamm, *Macromol. Rapid Commun.* **2004**, *25*, 360.
[20] N. Houbenov, S. Minko, M. Stamm, *Macromolecules* **2003**, *36*, 5897.

  